



Discover Generics

Cost-Effective CT & MRI Contrast Agents

 **FRESENIUS
KABI**

[WATCH VIDEO](#)

AJNR

**High-Spatial-Resolution MR Cisternography
of the Cerebellopontine Angle in 90 Seconds
with a Zero-Fill Interpolated Fast Recovery
3D Fast Asymmetric Spin-Echo Sequence**

Tatsuya Nakamura, Shinji Naganawa, Tokiko Koshikawa,
Hiroshi Fukatsu, Yasuo Sakurai, Ikuo Aoki, Ayako
Ninomiya and Takeo Ishigaki

This information is current as
of June 25, 2025.

AJNR Am J Neuroradiol 2002, 23 (8) 1407-1412
<http://www.ajnr.org/content/23/8/1407>

High-Spatial-Resolution MR Cisternography of the Cerebellopontine Angle in 90 Seconds with a Zero-Fill Interpolated Fast Recovery 3D Fast Asymmetric Spin-Echo Sequence

Tatsuya Nakamura, Shinji Naganawa, Tokiko Koshikawa, Hiroshi Fukatsu, Yasuo Sakurai, Ikuo Aoki, Ayako Ninomiya, and Takeo Ishigaki

BACKGROUND AND PURPOSE: Although the 12-minute 3D fast asymmetric spin-echo (FASE) protocol for imaging the inner ear has been satisfactory, reducing imaging time to minimize patient discomfort and maximize system throughput is desirable. We therefore evaluated the performance of a zero-fill interpolated (ZIP) fast recovery 3D FASE sequence in screening for cerebellopontine (CP) angle lesions in 90 seconds.

METHODS: Thirty consecutive patients known or suspected to have CP angle lesions underwent MR imaging at 1.5 T with use of bilateral quadrature phased-array coils designed for examination of the CP angle. Conventional 3D FASE images (4000/240/1 [TR/TE/NEX]) were obtained in 11 minutes 48 seconds with a field of view (FOV) of 16 cm, matrix of $512 \times 512 \times 40$, section thickness of 0.8 mm, and echo train length of 80. Then, ZIP fast recovery 3D FASE images (2000/240/1) were obtained in 90 seconds by using the same FOV. Contrast-enhanced T1-weighted 3D spoiled gradient-echo (SPGR) images were obtained as the reference standard. Three radiologists evaluated the images independently. Conventional 3D FASE and ZIP fast recovery 3D FASE images were reviewed at separate sessions.

RESULTS: On 3D SPGR images, 10 tumors were detected in 10 of the 30 patients. All lesions were depicted with both 3D FASE protocols. There were no false-positive results with either 3D FASE protocol. Both protocols showed 100% sensitivity and 100% specificity for all three reviewers.

CONCLUSION: High-spatial-resolution MR cisternography with the ZIP fast recovery 3D FASE protocol in 90 seconds results in a substantial reduction (by a factor of about eight) in the time required for screening for CP angle lesions compared with the previously reported conventional 3D FASE protocol, while maintaining high sensitivity and specificity.

High-spatial-resolution MR imaging of the inner ear with a heavily T2-weighted 3D fast asymmetric spin-echo (FASE) sequence with use of the half-Fourier technique has been performed successfully at 1.5 T (1). High sensitivity and specificity (100% and 99.8%, respectively) for the detection of cerebellopontine (CP) angle lesions with use of an approximately 12-minute imaging protocol with 3D FASE have been

reported (1). Recently, a fast recovery pulse was introduced and found to perform well at 1.5 T in various applications (2–5). Repetition time (TR) can be reduced while maintaining T2 contrast by applying a fast recovery pulse at the end of the echo train (6). Although the performance of the 12-minute protocol has been found to be satisfactory, reducing the imaging time to minimize patient discomfort and maximize system throughput is desirable. The purpose of the present study was to optimize and evaluate a protocol with a shorter imaging time by employing a fast recovery 3D FASE sequence at 1.5 T with zero-fill interpolation (ZIP) for the screening of CP angle lesions.

Methods

All imaging was performed with a 1.5-T whole-body MR imager (Visart/EX; Toshiba, Tokyo, Japan) by using bilateral

Received December 3, 2001; accepted after revision April 24, 2002.

From the Department of Radiology, Nagoya University School of Medicine, Japan (T.N., S.N., H.F., Y.S., T.I.); the Department of Radiology, Komaki City Hospital, Japan (T.K.); and Medical System Company, Toshiba Corporation, Tokyo, Japan (I.A., A.N.)

Address reprint requests to Shinji Naganawa, M.D., Department of Radiology, Nagoya University School of Medicine, 65 Tsurumai-cho, Shouwa-ku, Nagoya 466-8550, Japan.

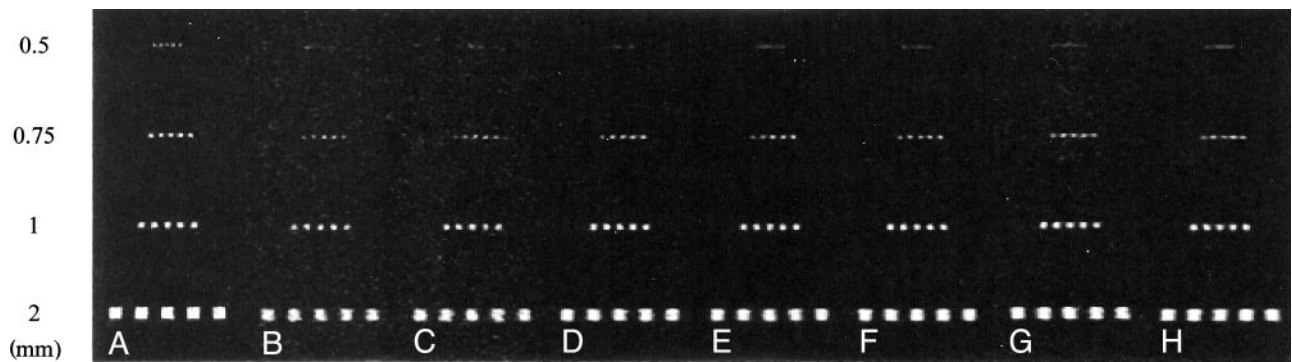


FIG 1. A–H, MR images of the phantom acquired with a conventional 3D FASE protocol (4000/4 [TR/number of shots], A) and seven fast recovery 3D FASE protocols (B–H): 1000/4 (B), 1500/2 (C), 2000/2 (D), 2500/2 (E), 3000/2 (F), 3000/1 (G), 4000/1 (H). Grids were aligned parallel to the phase-encoding direction, which has more blurring than the frequency direction. Note that protocols A, B, D, E, and F clearly depict the 0.75-mm grids separately. Only protocol A depicts the 0.5-mm grids separately.

quadrature phased-array coils designed for the examination of the CP angle.

Sequence Optimization

Initially, seven fast recovery 3D FASE protocols were used to obtain images of a phantom filled with distilled water (3D Resolution and Section Phantom; Nuclear Associates, New York, NY) and of a volunteer to determine the optimal TR and number of shots. In addition, a conventional 3D FASE protocol was used to obtain images of the water phantom and the volunteer. The phantom used contained grid elements 2.0, 1.0, 0.75, and 0.5 mm in width filled with distilled water, with the grid elements separated by intervals equal to their width. Each grid element was aligned parallel to the phase-encoding direction. The number of shots, which determines the echo train length (ETL), was varied from one to four. The number of shots corresponds to the number of excitation pulses used to cover the x-y plane of the k space for one section-encoding step. The parameters for the fast recovery 3D FASE protocols were varied as follows: one shot, an ETL of 128 with TR values of 3000 and 4000 ms; two shots, an ETL of 72 with TR values of 1500, 2000, 2500, and 3000 ms; and four shots, an ETL of 44 with a TR of 1000 ms. The echo spacing was 15.1 ms, and the effective echo time (TE) was set at 240 ms. The field of view (FOV) was 16 cm, with a 512×224 matrix (ZIP to 512×512) and a 1.6-mm section thickness (reconstructed at 0.8-mm intervals by ZIP). The parameters for the conventional 3D FASE protocol were as follows: four shots, an ETL of 80 with a TR of 4000 ms, TE of 240 ms, FOV of 16 cm, $512 \times 512 \times 40$ matrix, 0.8-mm section thickness, and imaging time of 11 minutes 48 seconds. The separation of the grid elements in phantom images was visually evaluated. On the volunteers' images, the contrast-to-noise ratio (C/N) between CSF and the cerebellum was measured at the level of the internal auditory canal. The C/N values in a given time were compared among the seven fast recovery 3D FASE protocols and the conventional 3D FASE protocol.

Patient Study

Thirty consecutive patients (15 men and 15 women; age range, 18–81 years; mean \pm SD, 53.0 ± 15.3 years) suspected or known to have CP angle lesions were included in this study during the study period from May 2000 to July 2001. They were referred by otologists to the MR department for follow-up of known CP angle lesions (six patients), for screening of suspected CP angle lesions on the basis of their otologic tests (12 patients), or for detailed study of suspected lesions on routine head MR images obtained at other hospitals (12 patients). Conventional 3D FASE images (4000/240/1 [TR/TE/NEX]) were obtained in 11 minutes 48 seconds with an FOV of 16 cm,

a matrix size of $512 \times 512 \times 40$, section thickness of 0.8 mm, and an ETL of 80 in four-shot mode. This protocol is the same as that previously reported (1). Then, ZIP fast recovery 3D FASE images (2000/240/1) were obtained in 90 seconds by using the same FOV, a matrix size of $512 \times 224 \times 20$ (ZIP to $512 \times 512 \times 40$, 0.8-mm section thickness), and an ETL of 72. The order of the two protocols was randomized. Nonenhanced and contrast material-enhanced (Magnevist; Nihon Schering, Nagoya City, Japan) T1-weighted 3D-spoiled gradient-echo (SPGR) imaging (23/10/1) was performed as the reference standard. For 3D SPGR imaging, a flip angle of 25° , $256 \times 224 \times 40$ matrix, 0.8-mm sections, and FOV of 16 cm were used. Three radiologists (T.N., S.N., T.K.) who were blinded to the patients' histories and symptoms evaluated the images independently, and visualization of the lesions was assessed and compared. The three radiologists had 2, 6, and 14 years, respectively, of experience in the field of neuroradiology. Images with conventional 3D FASE and ZIP fast recovery 3D FASE were reviewed at separate sessions. The two sessions were separated by at least 2 weeks. Visualization of CP angle lesions on each side was recorded as positive or negative.

The medical ethics committee of the university hospital approved the study protocol, and written informed consent was obtained from all participants.

Results

Sequence Optimization

In the phantom study, four of the seven fast recovery 3D FASE protocols and the conventional 3D FASE protocol enabled clear visualization of the 0.75-mm grid elements separately, whereas only the conventional 3D FASE protocol enabled visualization of the 0.5-mm grid elements separately (Fig 1).

The C/N values between CSF and the cerebellum in a given time were plotted as shown in Fig 2. The fast recovery protocols showed a higher C/N in a given time than that of the conventional 3D FASE protocol. Two-shot mode with TR values of 2000, 2500, and 3000 ms showed comparable C/N values in a given time. These three protocols enabled visualization of the 0.75-mm grid elements of the phantom separately. Among these TRs, a TR of 2000 ms allowed the widest slab coverage in a given time. This made it possible to cover a 32-mm slab in 90 seconds by using a 1.6-mm thickness. Thus, the two-shot mode with a TR of 2000 ms was used in this study (Fig 3).

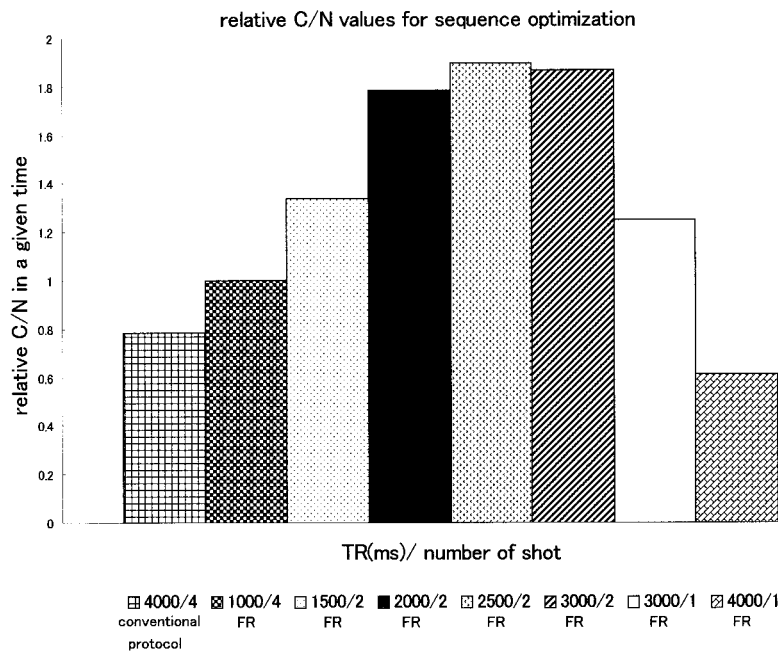


FIG 2. Relative C/N values between CSF and cerebellum in a given time in the volunteer study. The fast recovery (FR) 3D FASE protocols in two-shot mode with TRs of 2000, 2500, and 3000 ms show comparable C/N values in a given time. Among these TRs, a TR of 2000 ms allows the widest slab coverage in a given time. Thus, a TR of 2000 ms with two-shot mode was used in this study. Note that the C/N in a given time is higher in most of the fast recovery 3D FASE protocols than in the conventional protocol.

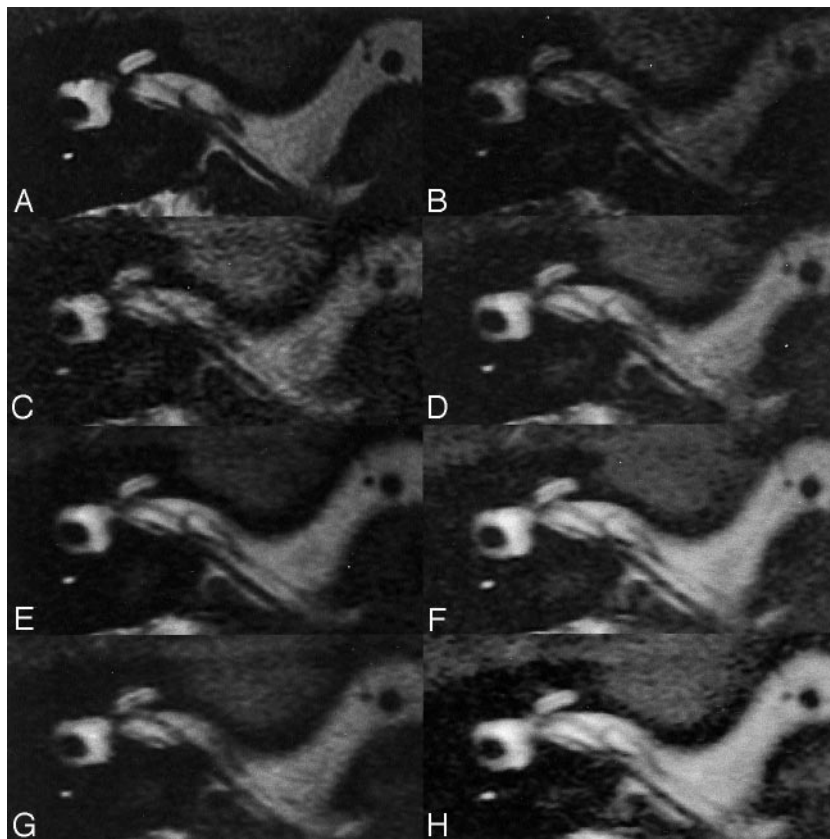


FIG 3. A-H, MR images acquired in the volunteer by means of a conventional 3D FASE protocol (4000/4 [TR/number of shots], A) and seven fast recovery 3D FASE protocols (B-H): 1000/4 (B), 1500/2 (C), 2000/2 (D), 2500/2 (E), 3000/2 (F), 3000/1 (G), 4000/1 (H).

Patient Study

On 3D SPGR images, 10 tumors were detected in 10 patients (Table). One was an intracanalicular superior vestibular nerve schwannoma measuring $1 \times 4 \times 3$ mm (Fig 4). Another was an intravestibular schwannoma measuring 3 mm in diameter (Fig 5). The other lesions were CP angle schwannomas, intracanalicular schwannomas, or CP angle meningio-

mas measuring 5–23 mm in diameter. All lesions were depicted with both 3D FASE protocols. There were no false-positive results with either 3D FASE protocol. In one patient in whom no lesion was seen on 3D SPGR images, the images acquired with the 12-minute protocol were slightly degraded by patient motion. However, the 90-second protocol was free of motion artifacts.

Lesion Characteristics

Patient No./Sex/Age (y)	Lesion	Location	Size (mm)
1/M/69	Schwannoma	Right CP angle	8 × 12 × 4
2/M/60	Schwannoma	Left IAC	1 × 4 × 3
3/F/58	Schwannoma	Left CP angle	20 × 10 × 12
4/M/57	Schwannoma	Right IAC	8 × 5 × 7
5/F/68	Schwannoma	Left IAC	5 × 5 × 6
6/F/67	Schwannoma	Right CP angle	18 × 16 × 14
7/F/53	Schwannoma	Right vestibular	3 × 3 × 3
8/F/70	Meningioma	Right CP angle	21 × 23 × 22
9/M/25	Schwannoma	Right CP angle	15 × 11 × 6
10/F/51	Schwannoma	Right CP angle	12 × 20 × 14

Note.— CP indicates cerebellopontine; IAC, internal auditory canal.

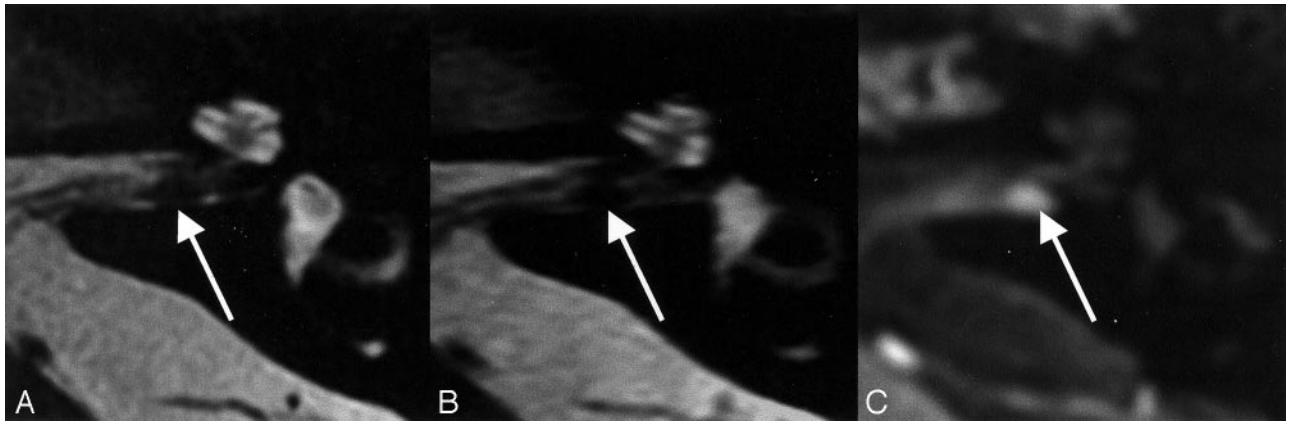


FIG 4. A–C, MR images show a small superior vestibular nerve schwannoma (arrow). The mass is clearly depicted with both 3D FASE protocols.

A, Conventional 3D FASE image (4000/240/1 [TR/TE/NEX]). Imaging time, 12 minutes.

B, ZIP fast recovery 3D FASE image (2000/240/1). Imaging time, 90 seconds.

C, Contrast-enhanced 3D-SPGR image (23/10/1).



FIG 5. A–C, MR images show a small intravestibular schwannoma (arrow). The mass is clearly depicted with both 3D FASE protocols.

A, Conventional 3D FASE image (4000/240/1). Imaging time, 12 minutes.

B, ZIP fast recovery 3D FASE image (2000/240/1). Imaging time, 90 seconds.

C, Contrast-enhanced 3D-SPGR image (23/10/1).

Discussion

In this study, we used contrast-enhanced 3D SPGR imaging as the standard of reference. In 10 of 30 patients, lesions presumed to be tumor were visualized. We do not have surgical proof in all patients, because their lesions were mostly small and the patients are being followed up or scheduled for radio-

surgery. Thus, lack of surgical proof is a limitation of this study.

The imaging time for the protocol in this study was set at 90 seconds. Of course, the imaging time could also be set to 2, 3, 4 minutes, and so on. If a 3-minute protocol were used, for example, the image quality would naturally be better than with a 90-second pro-

tol, assuming that the patient remains still during imaging. The reason that we selected a 90-second protocol is that this is the shortest imaging time that allows the inner ear apparatus and internal auditory canal to be covered with a 1.6-mm section thickness and a 512×224 matrix with a TR of 2000 ms and an ETL of 72, and this protocol also showed a high C/N in the volunteer study in terms of time efficiency.

The effective spatial resolution is higher for a conventional 12-minute protocol in either the phase-encoding or section-encoding direction, and further study is therefore necessary to determine whether the evaluation of cochlear nerve thickness to select candidates for cochlear implants is feasible by using the 90-second protocol. Cochlear fossa involvement by vestibular schwannoma is reported to be associated with a higher rate of unsuccessful hearing-preservation surgery (7). In the future, it will also be interesting to investigate whether the 90-second protocol is suitable for evaluating cochlear fossa involvement by vestibular schwannoma. In the present study, the smallest tumor measured 3 mm in diameter. We did not gather clinical data to evaluate the size of the smallest detectable tumor in the 90-second and 12-minute protocols. Some tumors much smaller than 3 mm may be detectable only by using the 12-minute protocol. However, in the phantom study, both protocols enabled visualization of the 0.75-mm grid elements separately, and we therefore assume that the minimum detectable tumor size by using these two protocols should not differ markedly. Furthermore, the growth rate of intracanalicular tumors is quite slow, as little as 0.2 mm/year (8). Thus, any difference in minimum detectable tumor size between the two protocols may not be significant in clinical practice, although further studies involving smaller tumors are necessary to prove this point. A reduction in imaging time would be expected to be particularly beneficial in the examination of pediatric patients, although no pediatric patients were included in the present study. At the very least, this 90-second protocol may prove to be useful as a backup for the 12-minute protocol if both protocols are employed sequentially.

The combination of a 3D fast spin-echo and the half-Fourier technique has been found to be quite successful for MR cisternography at 1.5 T (9). Gradient-echo-based sequences such as constructive interference in the steady state (CISS) (10), segment-interleaved motion-compensated acquisition in the steady state (SIMCAST) (11), and fully balanced steady-state coherent imaging (FBSSC) (12) have also been applied to the examination of the inner ear region. In particular, FBSSC is a 3D true fast imaging with steady-state precession (FISP)-type fast sequence that permits extremely short TR and TE values to be set if a high-performance gradient system is used. Even with the shorter TR and TE, these gradient-echo-based sequences are susceptible to flow ghosts from vessels and CSF and are more sensitive to field inhomogeneity than are fast spin-echo-based sequences (13). Furthermore, the specific absorption ratio of these sequences can be higher than that of 3D

fast spin-echo-based sequences (13). The specific absorption ratio limitation of these gradient-echo-based sequences would be significant at 3 T, although the single-slab 3D fast spin-echo sequence can satisfy the specific absorption ratio limitation even at 3 T (14) when head-coil radio-frequency transmission is used. Susceptibility artifacts may also be more pronounced at 3 T than at 1.5 T, especially with gradient-echo-based sequences.

A further reduction in imaging time can be achieved by using a sensitivity encoding (SENSE) technique, although this will result in a reduction in the signal-to-noise ratio in a given time (15).

Conclusion

High-spatial-resolution MR cisternography with use of the ZIP fast recovery 3D FASE sequence in 90 seconds results in a substantial reduction (by a factor of about eight) in the time required for screening for CP angle lesions compared with the previously reported conventional 3D FASE protocol, while maintaining high sensitivity and specificity.

References

1. Naganawa S, Ito T, Fukatsu H, et al. MR imaging of the inner ear: comparison of a three-dimensional fast spin-echo sequence with use of a dedicated quadrature-surface coil with a gadolinium-enhanced spoiled gradient-recalled sequence. *Radiology* 1998;208:679-685
2. Isogai S, Takehara Y, Isoda H, et al. **Kinematic MRI using short TR fast recovery single shot fast spin echo (FRSSFSE) in analyzing swallowing (abstr).** In: *Proceedings of the Eighth Meeting of the International Society for Magnetic Resonance in Medicine 2000*. Berkeley, CA: International Society for Magnetic Resonance in Medicine, 2000; 1120
3. Cheng D, Thibodeau S, Tan S, Tempany CMC. **Comparison of fast recovery fast spin echo and conventional fast spin echo for T2 weighted imaging of the prostate gland (abstr).** In: *Proceedings of the Eighth Meeting of the International Society for Magnetic Resonance in Medicine 2000*. Berkeley, CA: International Society for Magnetic Resonance in Medicine, 2000; 1436
4. Katayama M, Masui T, Kobayashi S, et al. **Fat-suppressed T2-weighted MR imaging of the liver: comparison of respiratory triggered fast spin-echo, breath-hold single-shot fast spin-echo and breath-hold fast-recovery fast spin-echo sequences (abstr).** In: *Proceedings of the Ninth Meeting of the International Society for Magnetic Resonance in Medicine 2001*. Berkeley, CA: International Society for Magnetic Resonance in Medicine, 2001; 235
5. Contreras M, Sica GT, Zou KH, et al. **T2-weighted MRI of the liver: comparison of fast recovery fast spin echo and single shot fast spin echo sequences (abstr).** In: *Proceedings of the Ninth Meeting of the International Society for Magnetic Resonance in Medicine 2001*. Berkeley, CA: International Society for Magnetic Resonance in Medicine, 2001; 2021
6. Kurucay S, Tan SG, Tanenbaum LN. **High resolution inner ear imaging with a fast recovery 3D fast spin echo sequence (abstr).** In: *Proceedings of the Seventh Meeting of the International Society for Magnetic Resonance in Medicine 1999*. Berkeley, CA: International Society for Magnetic Resonance in Medicine, 1999; 976
7. Dubrulle F, Ernst O, Vincent C, Vaneeckloo FM, Lejeune JP, Lemaitre L. **Cochlear fossa enhancement at MR evaluation of vestibular schwannoma: correlation with success at hearing-preservation surgery.** *Radiology* 2000;215:458-462
8. Walsh RM, Bath AP, Bance ML, Keller A, Tator CH, Rutka JA. **The role of conservative management of vestibular schwannomas.** *Clin Otolaryngol* 2000;25:28-29
9. Iwayama E, Naganawa S, Ito T, et al. **High-resolution MR cisternography of the cerebellopontine angle: 2D versus 3D fast spin-echo sequences.** *AJNR Am J Neuroradiol* 1999;20:889-895

10. Casselman JW, Kuhweide R, Deimling M, et al. **Constructive interference in steady state-3DFT MR imaging of the inner ear and cerebellopontine angle.** *AJNR Am J Neuroradiol* 1993;14:54-57
11. Kurucay S, Schmalbrock P, Chakeres DW, Keller PJ. **A segment-interleaved motion-compensated acquisition in the steady state (SIMCAST) technique for high resolution imaging of the inner ear.** *J Magn Reson Imaging* 1997;7:1060-1068
12. Vu AT. **High-resolution inner ear imaging using 3D asymmetric fully-balanced steady state coherent imaging pulse sequence (abstr).** In: *Proceedings of the Ninth Meeting of the International Society for Magnetic Resonance in Medicine 2001*. Berkeley, CA: International Society for Magnetic Resonance in Medicine, 2001; 1613
13. Naganawa S, Koshikawa T, Fukatsu H, et al. **MR cisternography of the cerebellopontine angle: comparison of 3D-FastASE and 3D-CISS sequences.** *AJNR Am J Neuroradiol* 2001;22:1179-1185
14. Naganawa S, Koshikawa T, Fukatsu H, et al. **Fast-recovery 3D-fast spin echo imaging of the inner ear at 3 T.** *AJNR Am J Neuroradiol* 2002;23:299-302
15. Pruessmann KP, Weiger M, Scheidegger MB, Boesiger P. **SENSE: sensitivity encoding for fast MRI.** *Magn Reson Med* 1999;42:952-962